Journal of Modern Applied Statistical Methods

Volume 17 | Issue 1 Article 12

6-19-2018

An Explanatory Study on the Non-Parametric Multivariate T2 Control Chart

Abdolrasoul Mostajeran
Department of Statistics, University of Isfahan, Isfahan, Iran, r.mostajeran@sci.ui.ac.ir

Nasrolah Iranpanah
Department of Statistics, University of Isfahan, Isfahan, Iran, iranpanah@sci.ui.ac.ir

Rassoul Noorossana
Industrial Engineering Department, Iran University of Science and Technology, Tehran, Iran, rassoul@iust.ac.ir

Recommended Citation
Mostajeran, A., Iranpanah, N., & Noorossana, R. (2018). An explanatory study on the non-parametric multivariate T2 control chart. Journal of Modern Applied Statistical Methods, 17(1), eP2559. doi: 10.22237/jmasm/1529418622

An Explanatory Study on the Non-Parametric Multivariate T2 Control Chart

Cover Page Footnote
The authors are grateful to the reviewers and editor in chief for their valuable comments which helped us to improve the quality of the manuscript. Also, the authors are grateful to the graduate office of the University of Isfahan for their support.

Journal of Modern Applied Statistical Methods
May 2018, Vol. 17, No. 1, eP2559
doi: 10.22237/jmasm/1529418622

ISSN 1538 − 9472

EMERGING SCHOLARS

An Explanatory Study on the Non-Parametric Multivariate T^2 Control Chart

A. Mostajeran
University of Isfahan
Isfahan, Iran

N. Iranpanah
University of Isfahan
Isfahan, Iran

R. Noorossana
Iran University of Science and Technology
Tehran, Iran

Most control charts require the assumption of normal distribution for observations. When distribution is not normal, one can use non-parametric control charts such as sign control chart. A deficiency of such control charts could be the loss of information due to replacing an observation with its sign or rank. Furthermore, because the chart statistics of T^2 are correlated, the T^2 chart is not a desire performance. Non-parametric bootstrap algorithm could help to calculate control chart parameters using the original observations while no assumption regarding the distribution is needed. In this paper, first, a bootstrap multivariate control chart is presented based on Hotelling's T^2 statistic then the performance of the bootstrap multivariate control chart is compared to a Hotelling's T^2 parametric multivariate control chart, a multivariate sign control chart, and a multivariate Wilcoxon control chart using a simulation study. Ultimately, the bootstrap multivariate control chart is used in an empirical example to study the process of sugar production.

Keywords: Non-parametric bootstrap, misspecified model, multivariate sign control chart, multivariate Wilcoxon control chart, average run length

Introduction

Statistical process control (SPC) is a proven method for improving quality of products and processes. Control chart is a featured tool of SPC which is very effective for controlling variability in manufacturing and service processes. Since a product ordinarily contains several quality characteristics, when a univariate control chart is used for monitoring product or process performance, misleading results due to ignoring the correlation between variables should be expected. Hotelling's T^2 control chart is one of the most important multivariate control

doi: 10.22237/jmasm/1529418622 | Accepted: March 21, 2017; Published: June 19, 2018.
Correspondence: Nasrollah Iranpanah, iranpanah@sci.ui.ac.ir

charts for monitoring the mean of a process. Shewhart and other multivariate control charts are usually based on the normality assumption of observations; however, in practice, this assumption might be violated. Thus, it will be suitable to use charts that are not based on normality assumption. In addition, it is often assumed that the F-distribution-based control limits account for the additional variability introduced into the T^2 statistics when the mean vector and covariance matrix are estimated. Because the chart statistics are correlated, the run length distribution of the T^2 chart is not a geometric distribution. Champ, Jones-Farmer, and Rigdon (2012) have shown that the F-distribution-based limits do not produce control charts with the desired in-control average run length (ARL_0) unless the sample sizes are very large. On the other hand, the non-parametric control charts do not require the normality assumption. Nonetheless, non-parametric control charts are based on the observations sign or rank, which are less efficient. In addition, the exact distributions of nonparametric control statistics are unknown and instead their limiting distributions are used for which the size of the recommended samples might not be large enough. In such cases, a bootstrap multivariate control chart could be used based on resampling the observations with no need for the normality assumption.

Bajgier (1992) presented a univariate control chart with limits obtained using the bootstrap method. Seppala, Moskowitz, Plante, and Tang (1995) improved the Bajgier control charts using subgroups bootstrap control charts. Liu and Tang (1996) presented a univariate bootstrap control chart for the mean of a process based on independent and dependent observations. The application of the bootstrap method in control charts based on discrete distributions using numerical integration was presented by Polansky (2005). Lio and Park (2008) suggested bootstrap control charts based on the Birnbaum-Saunders distribution. Park (2009) used bootstrap method to process median control charts. Chatterjee and Qiu (2009) presented a cumulative sum control chart in which the limits were obtained by the bootstrap method. Hotelling's T^2 multivariate bootstrap control chart for a process mean when a subgroup's sample size is one was first suggested by Phaladiganon, Kim, Chen, Baek, and Park (2011). They were also able to use the bootstrap method in multivariate control charts for principal component analysis based on non-normal distributions when subgroup size is one (Phaladiganon, Kim, Chen, & Jiang, 2013). Mostajeran, Iranpanah, and Noorossana (2016) proposed a new bootstrap algorithm to construct Hotelling's T^2 control chart for individual observations ($n = 1$).

The error caused by parameter estimation inevitably influences the chart performance. The effect of estimation error on control chart performance has been studied for various control charts. Jensen, Jones-Farmer, Champ, and Woodall (2006) studied effects of parameter estimation on control chart properties. Bischak and Trietsch (2007) investigated the rate of false signals in *X*-bar control charts with estimated limits. Castagliola, Celano, and Chen (2009) studied the exact run length distribution of the S^2 chart when the in-control variance is estimated. Mahmoud and Maravelakis (2010) discussed the performance of the MEWMA control chart when parameters are estimated. Saleh, Mahmoud, and Abdel-Salam (2013) studied the performance of the adaptive exponentially weighted moving average control chart with estimated parameters. Also, Mahmoud and Maravelakis (2013) discussed the performance of multivariate CUSUM control charts with estimated parameters. Lee, Wang, Xu, Schuh, and Woodall (2013) investigated the effect of parameter estimation on upper-sided Bernoulli cumulative sum charts. Psarakis, Vyniou, and Castagliola (2014) investigated some developments on the effects of parameter estimation on control charts. Jones-Farmer, Woodall, Steiner, and Champ (2014) discussed an overview of phase I analysis for process improvement and monitoring. Noorossana, Fathizadan, and Nayebpour (2015) investigated EWMA control chart performance with estimated parameters under non-normality. Aly, Saleh, Mahmoud, and Woodall (2015) studied the adaptive exponentially weighted moving average control chart when parameters are estimated. Epprecht, Loureiro, and Chakraborti (2015) discussed the effect of the amount of phase I data on the phase II performance of S^2 and S control charts. Recently, Saleh, Zwetsloot, Mahmoud, and Woodall (2016) investigated CUSUM charts with controlled conditional performance under estimated parameters. Faraz, Heuchenne, and Saniga (2017) proposed the *np* chart with guaranteed in-control average run lengths.

Bakir and Reynolds (1979) presented a cumulative sum control chart based on the Wilcoxon signed rank statistic. Chou, Mason, and Young (2001) proposed a control chart for individual observations from a multivariate non-normal distribution. The univariate non-parametric control charts were reviewed by Chakraborti, Van der Laan, and Bakir (2001) and Chakraborti, Human, and Graham (2008). Shewhart control charts based on the Wilcoxon sign rank statistic was first introduced by Bakir (2004). Albers and Kallenberg (2006) presented non-parametric control charts that use minimum subgroups instead of the mean of subgroups. In addition, Chakraborti and van de Weil (2008) developed the non-parametric control chart based on the Mann-Whitney statistic. Boone and Chakraborti (2012) presented the multivariate non-parametric Shewhart control charts based on observations' sign and ranks. Champ et al. (2012) investigated properties of the T^2 control chart when parameters are estimated.

Multivariate bootstrap control charts use subgroups of size one, but there are situations when subgroups of size greater than one are required. For the case of *m* subgroups of size *n*, there exists no suitable resampling algorithm in the literature. Many algorithms can be designed for resampling under this condition but the real challenge is the level of similarity between the algorithm and the original sampling idea. Obviously the more similar they are the more accurate data distribution will be established.

A bootstrap algorithm for Hotelling's T^2 chart when subgroup size is greater than one is presented. The bootstrap algorithm is used in a simulation study for comparing the bootstrap control chart with non-parametric sign control chart, Wilcoxon control chart, and Hotelling's T^2 control chart. The proposed algorithm was also used in an actual example in the process of sugar production from sugar beets.

Hotelling's T^2 Multivariate Control Chart

Assume $\mathbf{X}$ is a random vector that follows a *p*-variate normal distribution and $\mathbf{X}_1, \ldots, \mathbf{X}_n$ are i.i.d. random samples from $\mathrm{N}(\boldsymbol{\mu}_0, \boldsymbol{\Sigma}_0)$. The Hotelling's T^2 multivariate control chart for the process center is based on the statistic

$$T^2 = \mathrm{n}\left(\bar{\mathbf{X}} - \boldsymbol{\mu}_0\right)^{\mathrm{t}} \boldsymbol{\Sigma}_0^{-1} \left(\bar{\mathbf{X}} - \boldsymbol{\mu}_0\right)$$

where

$$\bar{\mathbf{X}} = \frac{1}{n}\sum_{j=1}^{n} \mathbf{X}_j$$

is the mean vector of the sample. Since the T^2 statistic has a chi-square distribution with *p* degrees of freedom, the multivariate Shewhart control chart for the process mean with known parameters mean vector $\boldsymbol{\mu}_0$ and covariance matrix $\boldsymbol{\Sigma}_0$ has upper control limit of $L_{\mathrm{u}} = \chi^2_{1-\alpha,p}$. In practice, both $\boldsymbol{\mu}_0$ and $\boldsymbol{\Sigma}_0$ are unknown and are estimated based on *m* random samples of size *n*. Suppose a sample $\mathbf{X}_{i1}, \ldots, \mathbf{X}_{in}$, $i = 1, \ldots, m$ in phase I with

$$\bar{\bar{\mathbf{X}}} = \frac{1}{m}\sum_{i=1}^{m} \bar{\mathbf{X}}_i \quad \text{and} \quad \bar{\mathbf{S}} = \frac{1}{m}\sum_{i=1}^{m} \mathbf{S}_i^2$$

is available where $\bar{\mathbf{X}}_i$ and $\mathbf{S}_i^2$ are the mean vector and covariance matrix for the i^{th} subgroup. In this case the Hotelling's T^2 control limit in phase II is based on statistic

$$T^2 = n\left(\bar{\mathbf{X}} - \bar{\bar{\mathbf{X}}}\right)^{t} \bar{\mathbf{S}}^{-1}\left(\bar{\mathbf{X}} - \bar{\bar{\mathbf{X}}}\right) \tag{1}$$

where $\bar{\mathbf{X}}$ is the mean vector of the sample mean in phase II.

Mason, Chou, and Young (2001) showed if the process has a normal distribution with p variables then T^2 / c will follow an F distribution with p and $mn - m - p + 1$ degrees of freedom, where $c = p(m + 1)(n - 1) / (mn - m - p + 1)$. The upper control limit for the p-variable Hotelling's T^2 is $L_u = cF_{1-\alpha,p,mn-m-p+1}$.

Nonparametric Multivariate Control Charts

The parametric multivariate control limit based on Hotelling's T^2 statistic in the previous section is based on the assumption that the p-variate vector of observations has a p-variable normal distribution. However, if such an assumption is not established, multivariate nonparametric control charts might be used. Two multivariate non-parametric control charts are presented which are based on the sign and rank of observations. Boone and Chakraborti (2012) presented the multivariate non-parametric Shewhart control charts based on the sign and rank of observations.

Multivariate Sign Control Chart

The multivariate sign control chart is based on the multivariate sign test. If the sign function is defined as

$$\text{sign}\left(X_{ij} - \theta_i\right) = \begin{cases} 1; & X_{ij} - \theta_i > 0 \\ 0; & X_{ij} - \theta_i = 0 \\ -1; & X_{ij} - \theta_i < 0 \end{cases}$$

where $\boldsymbol{\theta} = (\theta_1,\ldots, \theta_p)^t$ is the median vector, then for the i^{th} quality specification subject of the study, the sign test statistic is defined as

$$Z_i = \sum_{j=1}^{n} \text{sign}\left(X_{ij} - \theta_i\right), \quad i = 1,\ldots, p$$

The multivariate sign control chart for the process center is based on the statistic

$$T_S^2 = \mathbf{Z}^t \hat{\mathbf{V}}^{-1} \mathbf{Z} \tag{2}$$

where $\mathbf{Z} = (Z_1,\ldots, Z_p)^t$ is a sign vector and the matrix $\hat{\mathbf{V}}$ estimates the covariance matrix $\mathbf{V}$ as follows

$$\hat{\mathbf{V}}_{ii} = n,$$
$$\hat{\mathbf{V}}_{ij} = \sum_{k=1}^{n} \text{sign}\left(X_{ik} - \theta_i\right) \text{sign}\left(X_{jk} - \theta_j\right), \quad i, j = 1, 2,\ldots, p$$

Hettmansperger (1983) showed that when process is under control, by increasing the size of sample n, the distribution of T_S^2 is asymptotically distributed as chi-square with p degrees of freedom. Therefore, the upper limit for the non-parametric multivariate sign control chart is $L_u = \chi^2_{1-\alpha,p}$.

Multivariate Wilcoxon Signed-Rank Control Chart

The multivariate Wilcoxon signed-rank control chart is based on the multivariate Wilcoxon signed-rank test. For the i^{th} quality characteristic, we have

$$W_i = \sum_{j=1}^{n} \text{R}\left(\left|X_{ij} - \theta_i\right|\right) \text{sign}\left(X_{ij} - \theta_i\right), \quad i = 1,\ldots, p$$

where $\text{R}(|X_{ij} - \theta_i|)$ is the rank of $|X_{ij} - \theta_i|$ among $\{|X_{ij} - \theta_i|, \text{j} = 1,\ldots, n\}$. Therefore, W_i is the sum of the Wilcoxon signed-ranks for the i^{th} quality characteristic. If $\mathbf{W} = (W_1,\ldots, W_p)^t$ is a vector with covariance matrix estimated by $\hat{\mathbf{L}}$, defined by

$$\hat{l}_{ii} = \frac{n(n+1)(2n+1)}{6},$$

$$\hat{l}_{ij} = \sum_{k=1}^{n} \mathrm{R}\left(\left|X_{ik} - \theta_i\right|\right) \mathrm{R}\left(\left|X_{jk} - \theta_j\right|\right) \operatorname{sign}\left(X_{ik} - \theta_i\right) \operatorname{sign}\left(X_{jk} - \theta_j\right), \quad i, j = 1, 2, \ldots, p$$

then the Wilcoxon signed-rank chart statistic for the process center will be based on the statistic

$$T_{\mathrm{R}}^2 = \mathbf{W}^{\mathrm{t}} \hat{\mathbf{L}}^{-1} \mathbf{W} \tag{3}$$

Hettmansperger (1983) showed that when the process is under control, when sample size n increases, the distribution of T_{R}^2 is asymptotically distributed as chi-square with p degrees of freedom. Therefore, the upper control limit for the multivariate Wilcoxon signed-rank chart is given by $L_{\mathrm{u}} = \chi^2_{1-\alpha, p}$.

Bootstrap Multivariate Control Chart

In multivariate control charts based on Hotelling's T^2 statistic, the normality assumption is essential; however, in practice, this assumption could be violated most of the times. However, in non-parametric multivariate control charts, the control limits are based on the limiting distribution of the statistic while, in practice, the size of subgroup is small. In this part, an upper control limit in phase II is presented by using the bootstrap method based on resampling from observations in phase I with no need to use the assumption of normality for observations or the large subgroup size.

Suppose m random samples of size n on p quality characteristics are obtained in phase I. The different stages of the bootstrap algorithm for calculating the upper control limit are as follows:

1. Generate a simple random sample of size n, $\mathbf{X}_1^*, \ldots, \mathbf{X}_n^*$, by resampling from the observed p-variable sample vectors $\mathbf{X}_{ij}$: $i = 1, \ldots, m$, $j = 1, \ldots, n$ in phase I and define

$$\bar{\mathbf{X}}^* = \frac{1}{n} \sum_{j=1}^{n} \mathbf{X}_j^*$$

2. The bootstrap Hotelling's T^2 control statistic is presented as

$$T^{2*} = \mathrm{n}\left(\bar{\mathbf{X}}^{*} - \bar{\bar{\mathbf{X}}}^{*}\right)^{\mathrm{t}} \bar{\mathbf{S}}^{*-1}\left(\bar{\mathbf{X}}^{*} - \bar{\bar{\mathbf{X}}}^{*}\right) \tag{4}$$

   where $\bar{\bar{\mathbf{X}}}^{*}$ and $\bar{\mathbf{S}}^{*}$ are the mean vector and covariance matrix of a sample of size $m \times n$ generated by simple random sampling with replacement from the samples in phase I.
3. Repeat steps 1 and 2 for B times to calculate $T_1^{2*}, \ldots, T_B^{2*}$.
4. The bootstrap upper control limit is presented based on the empirical distribution of T^{2*} in $L_{\mathrm{u}} = T^{2*}_{\left[B(1-\alpha)\right]}$ form, in which $T^{2*}_{[b]}$ is the b^{th} percentile of the $T_1^{2*}, \ldots, T_B^{2*}$ bootstrap control statistic in step 2.

Use the established control limit to monitor new observations. In other words, if the statistic for the new observations exceeds L_{u}^{*}, we declare those observations as out-of-control signals.

Numerical Examples

Numerical examples are used to evaluate the performance of the proposed bootstrap multivariate control chart compared to the results obtained when multivariate parametric and non-parametric control charts are used. The average run length (ARL) is used as a criterion for performance evaluation. The control charts' ARL is the average number of observations prior to observing an out-of-control point. When a process is in-control, a false alarm rate (α) is used to calculate the in-control average run length, or ARL_0, as $\mathrm{ARL}_0 = 1 / \alpha$. Because the proposed bootstrap multivariate control chart is not dependent on the distribution, the simulation process is carried out using normal, T, skew-normal, and gamma distributions. For the two- and three-variable normal distribution, the mean vectors are defined as $\boldsymbol{\mu} = (0, 0)^{\mathrm{t}}$ and $\boldsymbol{\mu} = (0, 0, 0)^{\mathrm{t}}$, respectively, with the following covariance matrices:

$$\boldsymbol{\Sigma}_1 = \begin{bmatrix} 1 & 0.5 \\ 0.5 & 4.25 \end{bmatrix} \quad \text{and} \quad \boldsymbol{\Sigma}_2 = \begin{bmatrix} 1 & 0.5 & -1.5 \\ 0.5 & 4.25 & -1.75 \\ -1.5 & -1.75 & 2.99 \end{bmatrix}$$

In addition, in the two- and three-dimensional T distributions, the scale matrices are defined as $\mathbf{\Sigma}_1$ and $\mathbf{\Sigma}_2$, respectively, with two degrees of freedom. In the multivariate T distribution, the covariance matrix is given by $\text{cov}(\mathbf{X}) = \mathbf{\Sigma}(df / df - 2)$, where $\mathbf{\Sigma}$ is the shape matrix.

Azzalini (1985) proposed the univariate skew-normal distribution and it was generalized to the multivariate case by Azzalini and Dalla Valle (1996) and Arellano-Valle, Bolfarine, and Lachos (2005). The probability density function (pdf) of the generic element of a multivariate skew-normal distribution is given by

$$\text{f}_{\mathbf{Y}}(\mathbf{y}) = 2\phi_p(\mathbf{y} \mid \boldsymbol{\mu}, \mathbf{\Sigma})\Phi_1\left(\boldsymbol{\lambda}'\mathbf{\Sigma}^{-\frac{1}{2}}(\mathbf{y}-\boldsymbol{\mu})\right), \quad \mathbf{y} \in \mathbb{R}^p$$

where $\phi_p(\mathbf{y} \mid \boldsymbol{\mu}, \mathbf{\Sigma})$ stands for the pdf of the p-variate normal distribution with mean vector $\boldsymbol{\mu}$ and covariate matrix $\mathbf{\Sigma}$ and $\Phi_1(.)$ represents the cumulative distribution function (cdf) of the standard normal distribution. When $\lambda = 0$, the skew normal distribution reduces to the multivariate normal distribution. The skewness parameters $\boldsymbol{\lambda} = (-9, -6)$ and $\boldsymbol{\lambda} = (-9, -6, -3)$ have been used in the case of two and three variable response vectors, respectively.

To generate the multivariate data using a gamma distribution, let $\mathbf{y} = (y_0, y_1, \ldots, y_n)'$ be an $(n + 1)$ variate random vector and $y_i \sim \text{Ga}(\gamma_i, \alpha_i)$ be mutually independent gamma random variables possessing the pdfs

$$\text{f}_{y_i}(y) = \frac{\alpha_i^{\gamma_i}}{\Gamma(\alpha_i)} y^{\gamma_i - 1}\text{e}^{-\alpha_i y}, \quad y > 0$$

where $\gamma_i > 0$ and $\alpha_i > 0$ are the shape and rate parameters, respectively. Also let

$$\mathbf{A} = \begin{bmatrix} \frac{\alpha_0}{\alpha_1} & 1 & 0 & 0 & \cdots & 0 \\ \frac{\alpha_0}{\alpha_2} & \frac{\alpha_1}{\alpha_2} & 1 & 0 & \cdots & 0 \\ \frac{\alpha_0}{\alpha_3} & \frac{\alpha_1}{\alpha_3} & \frac{\alpha_2}{\alpha_3} & 1 & \cdots & 0 \\ \vdots & \vdots & \vdots & \vdots & \ddots & \vdots \\ \frac{\alpha_0}{\alpha_n} & \frac{\alpha_1}{\alpha_n} & \frac{\alpha_2}{\alpha_n} & \frac{\alpha_3}{\alpha_n} & \cdots & 1 \end{bmatrix}$$

Thus, $\mathbf{Ay} \sim \text{MG}\left(\bar{\boldsymbol{\gamma}}, \boldsymbol{\alpha}\right)$, where $\bar{\boldsymbol{\gamma}} = \left(\gamma_0 + \gamma_1, \gamma_0 + \gamma_1 + \gamma_2, \ldots, \gamma_0 + \ldots + \gamma_n\right)'$ and $\boldsymbol{\alpha} = (\alpha_1, \alpha_2, \ldots, \alpha_n)$ are the n-variate vectors of the shape and rate parameters, respectively (Furman, 2008).

In the case of two- and three-multivariate gamma distributions, we take $\boldsymbol{\gamma} = (0.5, 1.25, 2)'$ and $\boldsymbol{\gamma} = (0.5, 1.25, 2, 2.5)'$ as the shape parameters and $\boldsymbol{\alpha} = (0.01, 0.03, 0.04)'$ and $\boldsymbol{\alpha} = (0.01, 0.03, 0.04, 0.06)'$ as the rate parameters, respectively. The suggested bootstrap charts and non-parametric charts are implemented in R-3.3.1 software for our simulation study.

Empirical Distribution of T^{2*} Bootstrap Multivariate Statistic via Simulation

The empirical distribution of the bootstrap multivariate control statistic is studied in a simulated study. To study the bootstrap $T^{2}*$ statistic, plots based on the empirical distribution function are prepared. The data used in the simulation study are generated based on the three-variable normal, *T*, skew-normal, and gamma distributions.

In Figure 1, the Hotelling's T^2 values generated in phase II using relationship (1) are presented along with the Hotelling's T^2 three-dimensional upper control limit and the bootstrap $T^{2}*$ which is obtained in phase I. The phase I observations in this figure are generated using $m = 100$ samples of size $n = 10$ and the upper control limit for Hotelling's T^2 chart is obtained using $L_{\text{u}} = cF_{1-\alpha,v_1,v_2} = 7.9$, where v_1 and v_2 are equal to 3 and 898, respectively. In addition, the upper control limit $T^{2}*$ bootstrap is obtained based on the algorithm introduced in the previous section using the samples generated from each of the four distributions in phase I and bootstrap replications equal to 2000. Ultimately in phase II, 100 samples of size $n = 10$ are generated form each distribution, and the Hotelling's T^2 values in relationship (1) are calculated using $\bar{\bar{\mathbf{X}}}$ and $\bar{\mathbf{S}}$ as the estimators for population mean vector and covariance matrix. The estimates are computed using the observations generated in phase I.

As can be seen in Figure 1, when observations are generated from a normal distribution, the bootstrap upper control limit is very close to the upper control limit value of Hotelling's T^2 chart; however, in three other distributions, the upper control limits are not close. Therefore, we should expect the performance of a bootstrap control chart, in terms of false alarm rate, to be better than the simulated control charts, except the first one which is related to normal distribution.

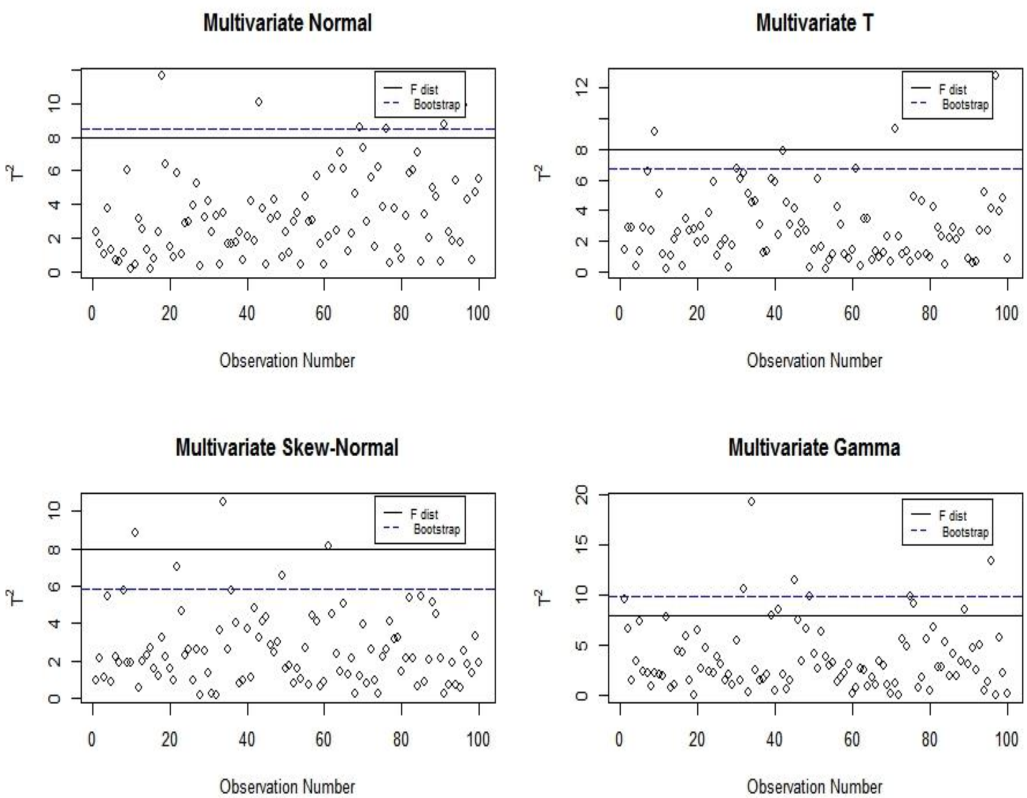

Figure 1. Hotelling's T^2 and T^{2*} bootstrap control charts with three-variables

---

In Figures 2 and 3, the boxplots and the cumulative distribution function of Hotelling's T^2 values, the data simulated from the F distribution, and the bootstrap T^{2*} control chart values are presented. First, in phase I, $m = 100$ samples, each with size $n = 10$ for three variables and four distributions, are generated and then the estimates of $\boldsymbol{\mu}_0$ and $\boldsymbol{\Sigma}_0$ are calculated using $\bar{\bar{\mathbf{X}}}$ and $\bar{\mathbf{S}}$. In phase II, $m = 1000$ samples of size $n = 10$ are simulated and the Hotelling's T^2 values are calculated using relationship (1). In addition, using random sampling with replacement, $m = 1000$ samples of size $n = 10$ are generated in phase I and using relationship (4); the values for bootstrap T^{2*} are calculated and plotted on the chart. To compare the performances of Hotelling's T^2 statistic distribution and the bootstrap T^{2*} distribution in normal and non-normal cases, 1000 observations from the F distribution with $v_1 = 3$ and $v_2 = 898$ degrees of freedom are generated, and graphs for Hotelling's T^2 chart and T^{2*} bootstrap chart are prepared.

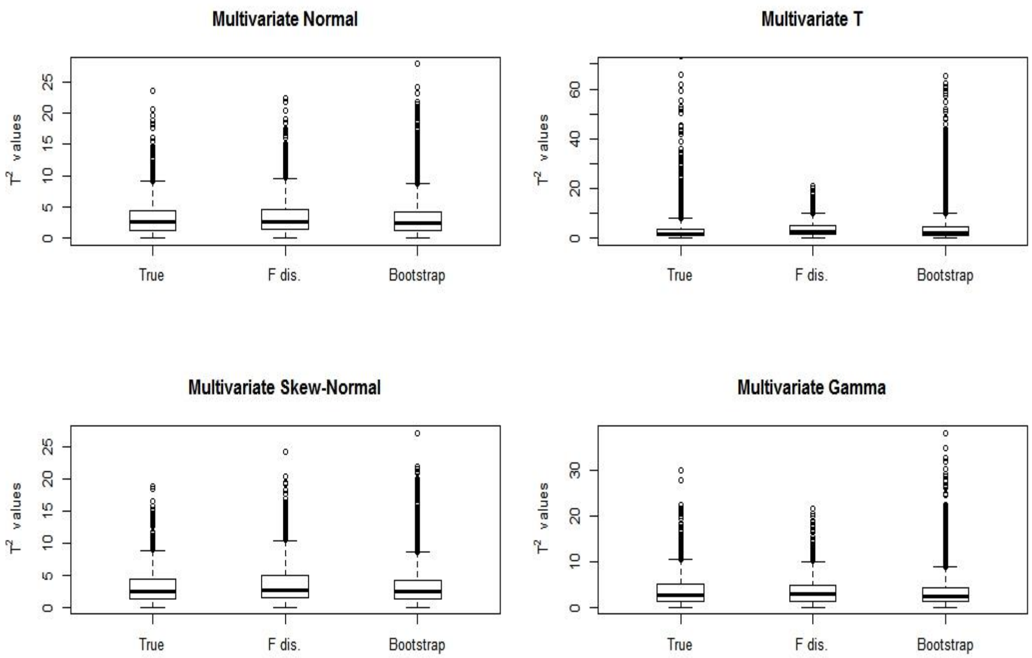

Figure 2. The boxplot of Hotelling's T^2 statistic, T^{2*} bootstrap statistic, and the simulated values from F distribution

In Figure 2, in the normal distribution, the boxplot of the bootstrap control statistic is similar to the Hotelling's T^2 boxplot. In all three boxplots related to the normal distribution, the first and third quartiles, interquartile ranges, and outlier observations are almost similar. In other distributions, as can be seen in Figure 2, the T^{2*} bootstrap control boxplot is closer to the Hotelling's T^2 plot. In fact, when the data do not follow a normal distribution, the T^{2*} bootstrap control boxplot is closer than the Hotelling's T^2 boxplot and is similar to the actual distribution in each figure.

In Figure 3, in the normal distribution, the cumulative distribution function of the bootstrap T^{2*} control chart is close to the Hotelling's T^2 cumulative distribution function. In other distributions, as Figure 3 shows, the bootstrap T^{2*}cumulative distribution function control chart is closer to the Hotelling's T^2 actual cumulative distribution than the F cumulative distribution function. In other words, when the distribution is not normal or is unknown, the bootstrap control chart estimates the Hotelling's T^2 distribution with more precision.

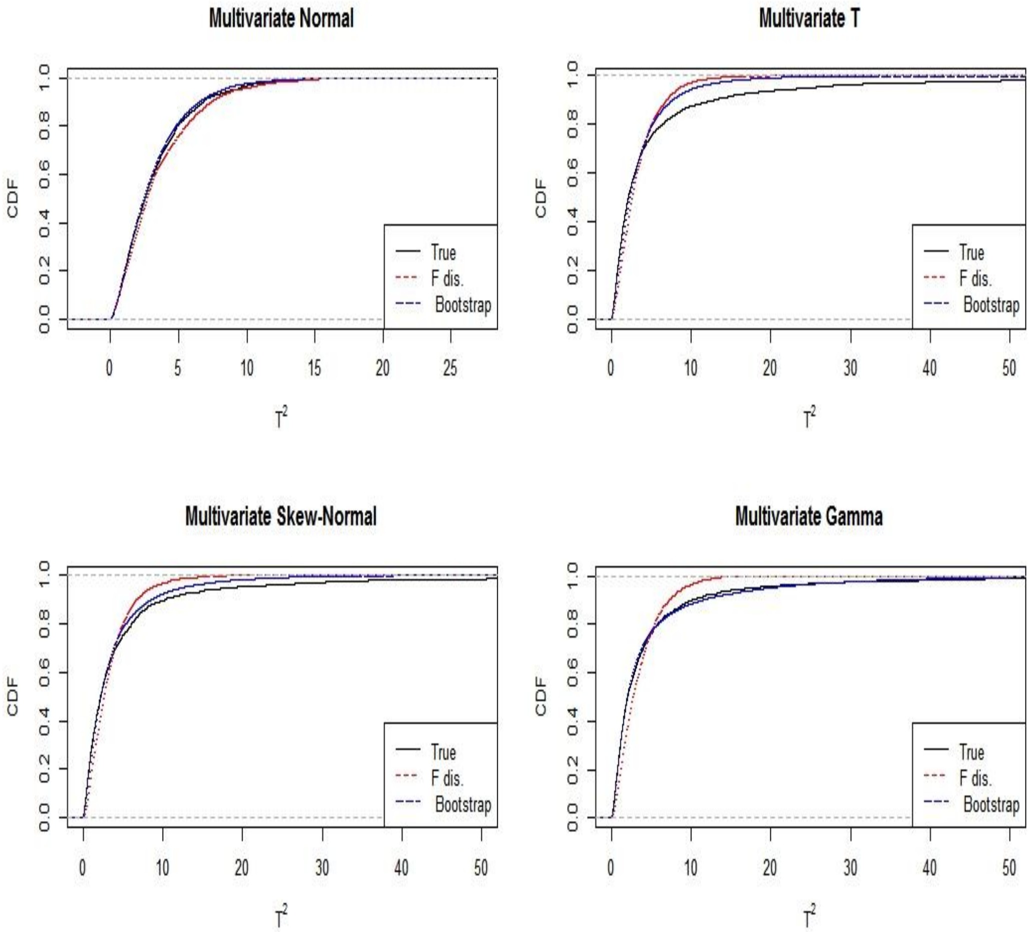

Figure 3. The empirical distribution function of Hotelling's T^2 control statistic, the empirical distribution function T^{2*} bootstrap, and the empirical distribution function based on F distribution

Comparison between the Bootstrap T^{2*} Control Charts and the Parametric and Non-Parametric Control Charts

To obtain a suitable bootstrap algorithm for resampling *m* samples of size *n*, 8 different algorithms were designed. In the basic stage, the algorithms were designed in simulated studies and the best bootstrap T^{2*} algorithm was selected to be compared with the Hotelling's T^2 chart and the non-parametric chart.

The ARL_0 is used in Monte Carlo simulations for comparing the performances of Hotelling's T^2 multivariate control charts, the sign non-parametric, the Wilcoxon non-parametric, and the bootstrap T^{2*}control chart. In order to do this, $m = 10$, 20 samples of size $n = 5$, 10 are generated from normal, *T*, skew-normal, and gamma distributions with two and three variables using the parameters presented in this section. An upper control limit for T^{2*} computed using the bootstrap method based on the algorithm introduced in the Bootstrap Multivariate Control Chart section with $B = 2000$ replications. The upper control limit for Hotelling's T^2 chart is calculated using $L_u = cF_{1-\alpha,p,mn-m-p+1}$, where $c = p(m + 1)(n - 1) / (mn - m - p + 1)$ for a given significance level. In addition, the upper control limit for the non-parametric sign and Wilcoxon charts, as shown in the Nonparametric Multi-Variate Control Charts section, are calculated based on *p* and the significance level alpha using $L_u = \chi^2_{1-\alpha,p}$. The simulated data in phase I is used to estimate the mean vector $\boldsymbol{\mu}_0$ and the covariance matrix $\boldsymbol{\Sigma}_0$ using $\bar{\bar{\mathbf{X}}}$ and $\bar{\mathbf{S}}$. In addition, the median vector was also calculated.

In phase II, *n* observations in the sample are used to generate data in order to calculate the Hotelling's T^2 statistic, the sign statistic from relationship (3), and the Wilcoxon statistic from relationship (4). The results are compared to the corresponding limits which were obtained in phase I. If the statistics are smaller than the limits, another set of *n* observations are produced and this process will be repeated until the statistic does not exceed the control limits. As soon as an observation plots out of control, the average run length criterion is computed. Phases I and II are repeated 10,000 times, and the in-control average run length, denoted by ARL_0 as, well as standard error of the run length (SDRL) are calculated. The values are presented in Tables 1 to 8 per each distribution, number of variables, number of samples, and the size of subgroups.

As can be seen from Tables 1 and 2 for the normal distribution case, the Hotelling's T^2 chart performs better than the other charts. In cases where the size of the subgroup is five, the ARL_0 value of the bootstrap control chart is in proximity to the nominal value and, even for two and three variables, on one occasion it is better than Hotelling's T^2 chart. Clearly, the non-parametric charts such as the Wilcoxon chart are far from the nominal ARL_0 value. Using the results in Table 2, the performance of the Wilcoxon chart in terms of ARL_0 gets worse as the subgroup size decreases from 10 to 5. In Tables 1 and 2, as one can see, the standard error of the bootstrap control chart is less than the other charts.

Table 1. ARL_0 values (SDRL in parenthesis) calculated by Hotelling's T^2, Sign chart, Wilcoxon chart, and bootstrap chart for normal distribution with p = 2 variables

			alpha = 0.005				**alpha = 0.01**			
		Chart	**T^2**	**Sign**	**W**	**Boot**	**T^2**	**Sign**	**W**	**Boot**
m	***n***	**TRUE**	**200**	**200**	**200**	**200**	**100**	**100**	**100**	**100**
10	5		**221.2**	264.0	491.8	174.0	112.1	69.3	231.3	**92.2**
			(257.0)	(271.2)	(489.3)	(198.1)	(136.2)	(62.3)	(237.3)	(104.7)
	10		**211.8**	157.5	230.8	178.1	**105.3**	109.6	85.5	92.1
			(242.9)	(152.4)	(244.3)	(186.0)	(111.2)	(105.7)	(85.9)	(96.8)
20	5		**211.6**	276.2	543.7	186.3	**101.1**	73.7	248.9	97.5
			(230.0)	(280.6)	(541.2)	(202.1)	(106.8)	(69.3)	(249.3)	(101.2)
	10		**206.1**	182.6	259.9	192.8	**102.9**	108.3	92.3	96.6
			(219.1)	(187.2)	(270.3)	(194.2)	(104.7)	(98.9)	(88.6)	(98.3)

Table 2. ARL_0 values (SDRL in parenthesis) calculated by Hotelling's T^2, Sign chart, Wilcoxon chart, and bootstrap chart for normal distribution with p = 3 variables

			alpha = 0.005				**alpha = 0.01**			
		Chart	**T^2**	**Sign**	**W**	**Boot**	**T^2**	**Sign**	**W**	**Boot**
m	***n***	**TRUE**	**200**	**200**	**200**	**200**	**100**	**100**	**100**	**100**
10	5		232.3	300.4	1547.9	**168.2**	114.6	175.9	254.9	**88.7**
			(266.9)	(306.1)	(1630.9)	(180.4)	(126.2)	(186.9)	(250.3)	(95.7)
	10		222.6	686.3	446.7	**177.9**	**109.1**	120.7	109.6	88.9
			(247.2)	(113.1)	(470.1)	(206.2)	(111.1)	(113.1)	(99.1)	(92.9)
20	5		**212.5**	331.1	1861.9	180.7	**101.2**	185.3	287.6	92.7
			(221.2)	(332.8)	(1951.8)	(189.6)	(100.2)	(185.2)	(289.1)	(92.0)
	10		**202.6**	795.6	521.8	187.2	**100.7**	129.9	119.3	95.4
			(213.3)	(784.9)	(545.7)	(176.8)	(98.6)	(126.5)	(118.8)	(93.1)

Table 3. ARL_0 values (SDRL in parenthesis) calculated by Hotelling's T^2, Sign chart, Wilcoxon chart, and bootstrap chart for T distribution with p = 2 variables

			alpha = 0.005				**alpha = 0.01**			
		Chart	**T^2**	**Sign**	**W**	**Boot**	**T^2**	**Sign**	**W**	**Boot**
m	***n***	**TRUE**	**200**	**200**	**200**	**200**	**100**	**100**	**100**	**100**
10	5		126.9	264.7	639.6	**251.2**	91.1	69.3	253.2	**108.3**
			(225.1)	(282.1)	(659.1)	(366.8)	(178.1)	(66.1)	(259.3)	(210.5)
	10		130.3	170.2	247.2	**214.2**	107.4	103.6	90.2	**97.1**

			(213.2)	(173.0)	(252.8)	(405.1)	(141.5)	(97.8)	(86.4)	(138.3)
20	5		142.9	290.5	709.8	**244.9**	**110.2**	77.9	318.6	112.3
			(275.7)	(280.8)	(742.3)	(461.9)	(211.9)	(72.9)	(315.5)	(109.4)
	10		136.1	185.9	287.8	**221.6**	108.9	111.4	103.1	**102.9**
			(168.8)	(197.2)	(281.6)	(322.1)	(178.2)	(109.8)	(97.7)	(160.1)

Based on the results presented in Table 3 for the T distribution, the bootstrap control chart is better than Hotelling's T^2 chart and the non-parametric charts; however, in three cases, its standard error is bigger than the other chart. Based on the results in Table 4, the ARL_0 value of the bootstrap control chart is closer to the desirable value, specifically for $\alpha = 0.005$. The ARL_0 values of Hotelling's T^2 chart are in all cases lower than the nominal value with low standard error. In fact, when the data distribution follows a T distribution, Hotelling's T^2 chart yields large false alarm rate.

Table 4. ARL_0 values (SDRL in parenthesis) calculated by Hotelling's T^2, Sign chart, Wilcoxon chart, and bootstrap chart for T distribution with p = 3 variables

			alpha = 0.005				**alpha = 0.01**			
		Chart	**T^2**	**Sign**	**W**	**Boot**	**T^2**	**Sign**	**W**	**Boot**
m	***n***	**TRUE**	**200**	**200**	**200**	**200**	**100**	**100**	**100**	**100**
10	5		86.5	314.4	1910.1	**221.2**	66.5	170.2	282.6	**92.1**
			(127.4)	(318.9)	(2132.1)	(244.3)	(84.2)	(165.9)	(278.5)	(118.2)
	10		97.4	689.1	521.7	**196.6**	67.3	119.1	115.7	**103.3**
			(124.2)	(722.4)	(570.2)	(452.5)	(84.7)	(118.0)	(116.6)	(107.4)
20	5		108.5	342.0	2319.1	**194.7**	81.3	183.9	319.0	**109.1**
			(137.4)	(352.3)	(2408.0)	(273.4)	(113.8)	(185.0)	(326.9)	(130.4)
	10		111.6	775.5	621.6	**189.1**	76.6	138.7	133.3	**105.0**
			(127.2)	(789.4)	(668.0)	(235.9)	(111.4)	(131.6)	(127.8)	(123.1)

Table 5. ARL_0 values (SDRL in parenthesis) calculated by Hotelling's T^2, Sign chart, Wilcoxon chart, and bootstrap chart for skew-normal distribution with p = 2 variables

			alpha = 0.005				**alpha = 0.01**			
		Chart	**T^2**	**Sign**	**W**	**Boot**	**T^2**	**Sign**	**W**	**Boot**
m	***n***	**TRUE**	**200**	**200**	**200**	**200**	**100**	**100**	**100**	**100**
10	5		256.9	262.6	444.7	**194.9**	128.9	71.2	200.2	**99.4**
			(361.5)	(262.4)	(467.8)	(213.4)	(152.7)	(67.1)	(205.1)	(117.5)
	10		258.6	162.3	218.1	**191.1**	115.3	91.1	83.4	**92.5**
			(282.6)	(165.9)	(215.8)	(209.0)	(121.5)	(90.6)	(82.9)	(96.3)
20	5		235.7	292.9	483.9	**196.6**	117.1	71.2	217.1	**98.4**
			(260.0)	(292.3)	(483.7)	(213.1)	(118.3)	(68.8)	(213.3)	(100.7)
	10		226.9	186.7	242.5	**195.4**	109.8	106.3	90.6	**96.2**
			(258.8)	(191.0)	(247.1)	(197.1)	(107.8)	(105.2)	(89.8)	(95.3)

Table 6. ARL_0 values (SDRL in parenthesis) calculated by Hotelling's T^2, Sign chart, Wilcoxon chart, and bootstrap chart for skew-normal distribution with p = 3 variables

			alpha = 0.005				**alpha = 0.01**			
		Chart	T^2	**Sign**	**W**	**Boot**	T^2	**Sign**	**W**	**Boot**
m	***n***	**TRUE**	**200**	**200**	**200**	**200**	**100**	**100**	**100**	**100**
10	5		247.8	316.7	1234.1	**191.4**	125.3	155.9	243.2	**92.8**
			(310.5)	(316.5)	(1270.2)	(207.8)	(136.7)	(153.7)	(254.1)	(99.7)
	10		238.6	619.3	446.7	**178.4**	110.9	119.1	109.5	**92.5**
			(262.3)	(679.3)	(452.3)	(196.3)	(116.9)	(117.9)	(105.6)	(92.0)
20	5		221.2	334.5	1421.2	**188.7**	109.2	169.5	257.0	**94.6**
			(235.9)	(331.9)	(1459.9)	(190.8)	(109.6)	(163.6)	(261.2)	(96.5)
	10		216.7	683.2	484.9	**189.4**	116.3	127.2	123.1	**96.2**
			(225.3)	(695.7)	(493.7)	(196.4)	(111.7)	(119.8)	(118.7)	(94.5)

Table 7. ARL_0 values (SDRL in parenthesis) calculated by Hotelling's T^2, Sign chart, Wilcoxon chart, and bootstrap chart for gamma distribution with p = 2 variables

			alpha = 0.005				**alpha = 0.01**			
		Chart	T^2	**Sign**	**W**	**Boot**	T^2	**Sign**	**W**	**Boot**
m	***n***	**TRUE**	**200**	**200**	**200**	**200**	**100**	**100**	**100**	**100**
10	5		265.2	277.2	428.6	229.1	136.9	77.1	229.6	110.9
			(419.7)	(274.4)	(470.1)	(322.4)	(197.7)	(72.3)	(238.3)	(152.1)
	10		254.5	186.3	168.4	196.8	120.6	140.6	72.1	97.4
			(359.5)	(183.5)	(198.2)	(256.2)	(143.5)	(144.4)	(71.9)	(113.8)
20	5		219.7	295.5	444.1	209.3	118.6	82.7	234.3	103.1
			(256.8)	(291.3)	(455.9)	(238.9)	(137.9)	(76.9)	(239.2)	(113.7)
	10		220.8	209.3	181.6	208.1	111.8	147.1	77.1	98.1
			(257.3)	(206.1)	(184.6)	(217.9)	(115.4)	(144.6)	(77.9)	(97.0)

Table 8. ARL_0 values (SDRL in parenthesis) calculated by Hotelling's T^2, Sign chart, Wilcoxon chart, and bootstrap chart for gamma distribution with p = 3 variables

			alpha = 0.005				**alpha = 0.01**			
		Chart	T^2	**Sign**	**W**	**Boot**	T^2	**Sign**	**W**	**Boot**
m	***n***	**TRUE**	**200**	**200**	**200**	**200**	**100**	**100**	**100**	**100**
10	5		239.3	307.4	1397.1	208.7	118.6	170.1	217.1	99.3
			(290.3)	(301.5)	(1410.1)	(280.4)	(141.5)	(166.7)	(219.6)	(126.6)
	10		222.5	699.9	344.8	197.4	116.7	123.7	82.7	94.5
			(281.8)	(762.9)	(389.0)	(247.4)	(131.9)	(126.4)	(91.1)	(101.2)
20	5		208.5	349.6	1571.2	196.1	111.4	186.2	247.1	101.8

	(228.5)	(348.9)	(1629.2)	(223.6)	(116.4)	(181.7)	(255.7)	(100.1)
10	218.9	750.3	384.6	202.7	109.6	139.2	92.1	96.6
	(261.2)	(755.9)	(406.9)	(215.2)	(111.2)	(134.3)	(91.0)	(94.9)

According to the results in Tables 5 and 6, in almost all cases, the bootstrap control chart performs better than Hotelling's T^2 chart and the non-parametric charts. For $\alpha = 0.005$, Hotelling's T^2 chart had a relatively acceptable performance by considering the fact that the skew-normal distribution is similar to the normal distribution; however, the standard error of ARL_0 vales for the T^2 Hotelling chart is greater than the bootstrap control chart.

Based on the results in Tables 7 and 8, the bootstrap control chart is better than Hotelling's T^2 chart and the non-parametric charts. In fact, in all cases, the ARL_0 value for the bootstrap control chart is close to the nominal value. This is particularly obvious for $\alpha = 0.005$. In fact, when observations follow a gamma distribution, using non-parametric charts would increase the number of defective products due to the low number of out-of-control alarms. In other words, the non-parametric control charts wrongly indicate an out-of-control process as an in-control process. The ARL_0 values which are presented in Tables 1 through 8 and their corresponding boxplots, which are presented in Figure 4 to 7, show (from left to right) Hotelling's T^2 control chart, sign chart, Wilcoxon chart, and the bootstrap chart. The normal, *T*, skew-normal, and gamma distributions are considered for two variables using alpha levels of 0.01 and 0.005. The size of subgroups used are $n = 5$, 10, the number of samples taken are $m = 10$, 20. The number of bootstrap replications is 2,000 and the number of Monte Carlo simulation iterations is 10,000.

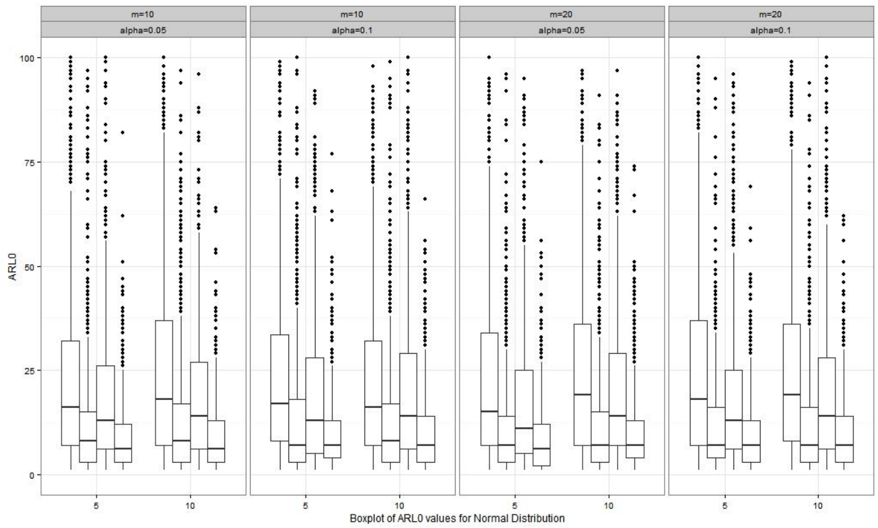

Figure 4. The boxplots of ARL_0 values for a bivariate normal distribution and Hotelling's T^2, Sign chart, Wilcoxon chart, and bootstrap chart

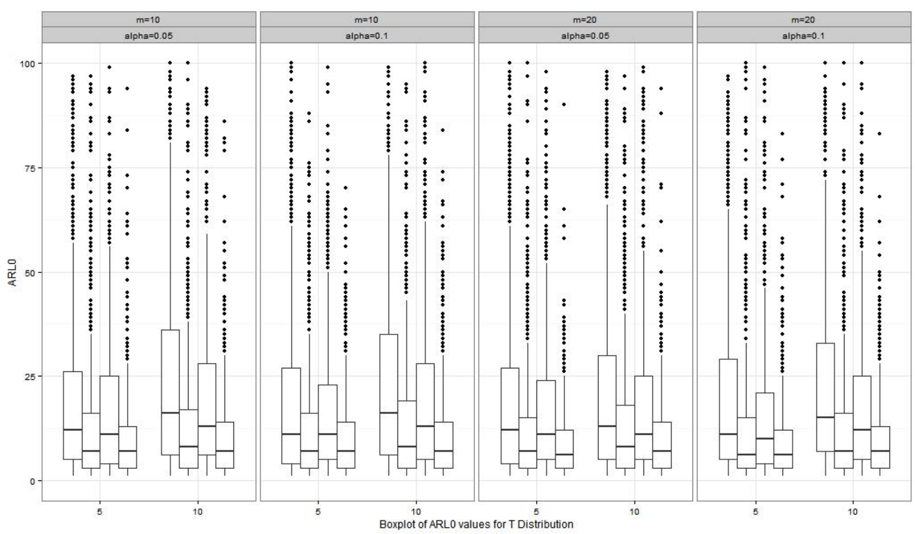

Figure 5. The boxplots of ARL_0 values for a bivariate T distribution and Hotelling's T^2, Sign chart, Wilcoxon chart, and bootstrap chart

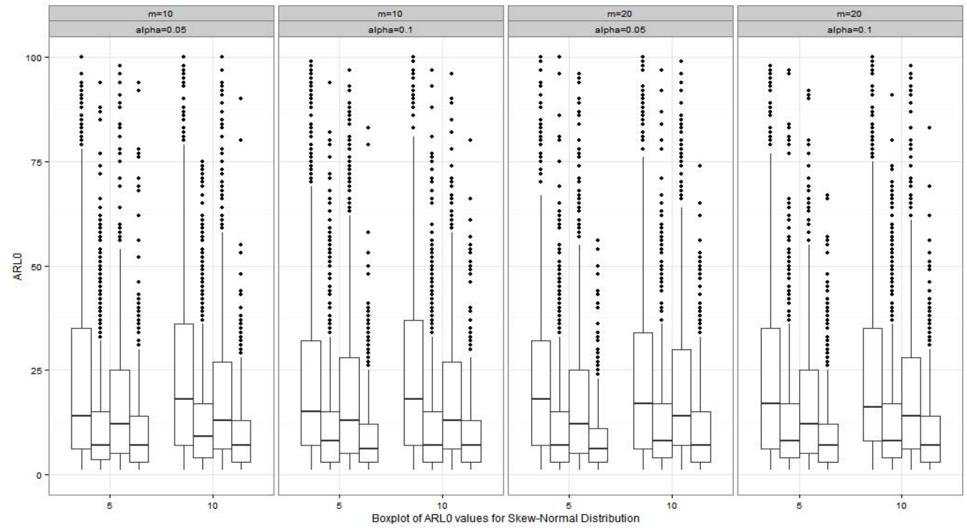

Figure 6. The boxplots of ARL_0 values for a bivariate skew-normal distribution and Hotelling's T^2, Sign chart, Wilcoxon chart, and bootstrap chart

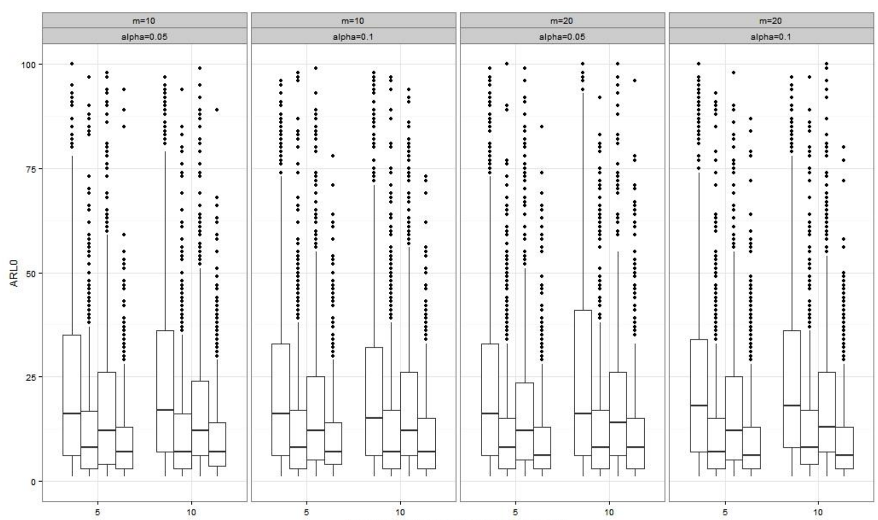

Figure 7. The boxplots of ARL_0 values for a bivariate gamma distribution and Hotelling's T^2, Sign chart, Wilcoxon chart, and bootstrap chart

The interquartile range (IQR) of Hotelling's T^2 chart and the Wilcoxon chart are bigger than the sign and bootstrap charts. The IQR of the bootstrap charts are smaller than the other charts for all distributions. Furthermore, the number of outliers is smaller than the other charts.

A Real Data Example

Several factors are important in the production process of sugar from the sugar beet. The juice extracted from beets is converted to sugar after a number of chemical processes. Two of the most important variables in this process are the Brix number (the amount of solid particles in the juice solution) and pH of the solution; both affect the quality of the sugar obtained from the beet juice. A dataset obtained from Isfahan sugar factory contains the Brix number and pH of the diluted juice, recorded six times a day for 20 days. First, the normality of the data was tested by using the Mardia test (Mardia, 1980) and the probability value was obtained to be less than 0.0001, which strongly rejects the assumption of normality.

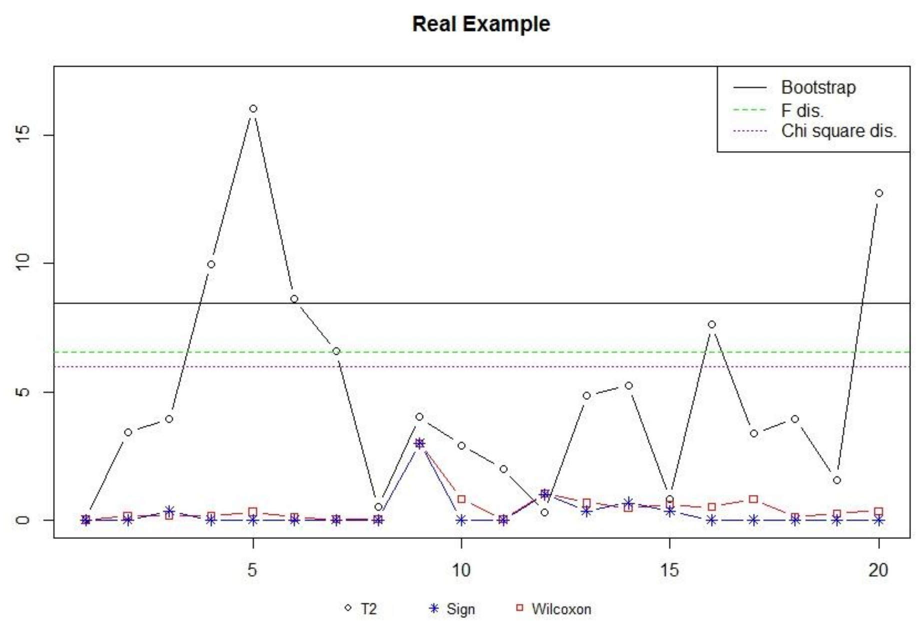

Figure 8. Plot of bootstrap, Hotelling's T^2, and non-parametric control charts

The upper limit of bootstrap control chart was obtained using 2,000 replications of the Brix and pH of the diluted juice, as well as the upper limits of Hotelling's T^2 and the sign and Wilcoxon non-parametric charts. The Hotelling's T^2, sign, and Wilcoxon statistics and the corresponding control limits are drawn in Figure 8. As Figure 8 shows, the control limit of the bootstrap chart is significantly different than the control limit of Hotelling's T^2 chart and the control limits of the non-parametric charts. The non-parametric statistics obtained from samples reveal that the samples are under control, while the Hotelling's T^2 chart show six samples to be out-of-control, and the bootstrap chart shows four samples to be out-of-control.

Conclusion

In general, the non-parametric charts are sensitive to subgroup size, that is, as the size of sample decreases, the non-parametric chart performance deteriorates. The non-parametric charts usually require a large amount of sample size subgroups while, in practice, the size of the sample is small. Hotelling's T^2 chart does not have the required efficiency in misspecified models.

Here, work on the T^2 chart was extended, especially pertaining to Phaladiganon et al. (2011), by considering $n > 1$ (when subgroup sample size is greater than one). A recently proposed non-parametric algorithm was described to be used in designing the T^2 chart. This procedure enables practitioners to achieve the desired in-control performance using the available phase I data. However, the non-parametric bootstrap control chart, which is presented in this paper for Hotelling's T^2, statistic does not depend on the observations' distribution. That is, if a non-parametric bootstrap is applied, the approach is robust against model misspecification. This fact was studied and presented in simulation studies. The bootstrap control chart performs fairly well when the size of subgroups is small.

References

Albers, W., & Kallenberg, W. C. (2006). *Control charts using minima instead of averages*. Unpublished manuscript. Department of Applied Mathematics, University of Twente, The Netherlands. Retrieved from https://ris.utwente.nl/ws/portalfiles/portal/5518717

Aly, A. A., Saleh, N. A., Mahmoud, M. A., & Woodall, W. H. (2015). A reevaluation of the adaptive exponentially weighted moving average control chart when parameters are estimated. *Quality and Reliability Engineering International*, *31*(8), 1611-1622. doi: 10.1002/qre.1695

Arellano-Valle, R., Bolfarine, H., & Lachos, V. (2005). Skew-normal linear mixed models. *Journal of Data Science, 3*(4), 415-438. Retrieved from http://www.jds-online.com/v3-4

Azzalini, A. (1985). A class of distributions which includes the normal ones. *Scandinavian Journal of Statistics*, *12*(2), 171-178. Available from http://www.jstor.org/stable/4615982

Azzalini, A., & Dalla Valle, A. (1996). The multivariate skew-normal distribution. *Biometrika*, *83*(4), 715-726. doi: 10.1093/biomet/83.4.715

Bajgier, S. M. (1992). The use of bootstrapping to construct limits on control charts. In *Proceedings of the Decision Sciences Institute* (pp. 1611-1613). Atlanta, GA: Decision Sciences Institute.

Bakir, S. T. (2004). A distribution-free Shewhart quality control chart based on signed-ranks. *Quality Engineering*, *16*(4), 613-623. doi: 10.1081/qen-120038022

Bakir, S. T., & Reynolds, M. R. (1979). A nonparametric procedure for process control based on within-group ranking. *Technometrics*, *21*(2), 175-183. doi: 10.1080/00401706.1979.10489747

Bischak, D., & Trietsch, D. (2007). The rate of false signals in $\bar{U}$ control charts with estimated limits. *Journal of Quality Technology*, *39*(1), 54-65. doi: 10.1080/00224065.2007.11917673

Boone, J., & Chakraborti, S. (2012). Two simple Shewhart-type multivariate nonparametric control charts. *Applied Stochastic Models in Business and Industry*, *28*(2), 130-140. doi: 10.1002/asmb.900

Castagliola, P., Celano, G., & Chen, G. (2009). The exact run length distribution and design of the S^2 chart when the in-control variance is estimated. *International Journal of Reliability, Quality and Safety Engineering*, *16*(01), 23-38. doi: 10.1142/s0218539309003277

Chakraborti, S., Human, S. W., & Graham, M. A. (2008). Phase I statistical process control charts: an overview and some results. *Quality Engineering*, *21*(1), 52-62. doi: 10.1080/08982110802445561

Chakraborti, S., & van de Wiel, M. A. (2008). A nonparametric control chart based on the Mann-Whitney statistic. *Institute of Mathematical Statistics, 1*, 156-172. doi: 10.1214/193940307000000112

Chakraborti, S., Van Der Laan, P., & Bakir, S. (2001). Nonparametric control charts: An overview and some results. *Journal of Quality Technology, 33*(3), 304-315. doi: 10.1080/00224065.2001.11980081

Champ, C. W., Jones-Farmer, L. A., & Rigdon, S. E. (2012). Properties of the T^2 control chart when parameters are estimated. *Technometrics*, *47*(4), 437-445. doi: 10.1198/004017005000000229

Chatterjee, S., & Qiu, P. (2009). Distribution-free cumulative sum control charts using bootstrap-based control limits. *The Annals of Applied Statistics*, *3*(1), 349-369. doi: 10.1214/08-aoas197

Chou, Y.-M., Mason, R. L., & Young, J. C. (2001). The control chart for individual observations from a multivariate non-normal distribution. *Communications in Statistics – Theory and Methods*, *30*(8-9), 1937-1949. doi: 10.1081/sta-100105706

Epprecht, E. K., Loureiro, L. D., & Chakraborti, S. (2015). Effect of the amount of phase I data on the phase II performance of S^2 and *S* control charts. *Journal of Quality Technology*, *47*(2), 139-155. doi: 10.1080/00224065.2015.11918121

Faraz, A., Heuchenne, C., & Saniga, E. (2017). The *np* chart with guaranteed in-control average run lengths. *Quality and Reliability Engineering International*, *33*(5), 1057-1066. doi: 10.1002/qre.2091

Furman, E. (2008). On a multivariate gamma distribution. *Statistics & Probability Letters, 78*(15), 2353-2360. doi: 10.1016/j.spl.2008.02.012

Hettmansperger, T. (1982). Multivariate location tests. In S. Kotz & N. L. Johnson (Eds.), *Encyclopedia of statistical sciences* (Vol. 6) (pp. 79-83). New York, NY: Wiley.

Jensen, W. A., Jones-Farmer, L. A., Champ, C. W., & Woodall, W. H. (2006). Effects of parameter estimation on control chart properties: A literature review. *Journal of Quality Technology*, *38*(4), 349-364. doi: 10.1080/00224065.2006.11918623

Jones-Farmer, L. A., Woodall, W. H., Steiner, S. H., & Champ, C. W. (2014). An overview of phase I analysis for process improvement and monitoring. *Journal of Quality Technology*, *46*(3), 265-280. doi: 10.1080/00224065.2014.11917969

Lee, J., Wang, N., Xu, L., Schuh, A., & Woodall, W.H. (2013). The effect of parameter estimation on upper-sided Bernoulli cumulative sum charts. *Quality and Reliability Engineering International*, *29*(5), 639-651. doi: 10.1002/qre.1413

Lio, Y., & Park, C. (2008). A bootstrap control chart for Birnbaum-Saunders percentiles. *Quality and Reliability Engineering International, 24*(5), 585-600. doi: 10.1002/qre.924

Liu, R. Y., & Tang, J. (1996). Control charts for dependent and independent measurements based on bootstrap methods. *Journal of the American Statistical Association, 91*(436), 1694-1700. doi: 10.1080/01621459.1996.10476740

Mahmoud, M. A., & Maravelakis, P. E. (2010). The performance of the MEWMA control chart when parameters are estimated. *Communications in Statistics – Simulation and Computation, 39*(9), 1803-1817. doi: 10.1080/03610918.2010.518269

Mahmoud, M., & Maravelakis, P. (2013). The performance of multivariate CUSUM control charts with estimated parameters. *Journal of Statistical Computation and Simulation, 83*(4), 721-738. doi: 10.1080/00949655.2011.633910

Mardia, K. V. (1980). 9 tests of unvariate and multivariate normality. In P. R. Krishnaiah (Ed.), *Handbook of statistics* (Vol. 1) (pp. 279-320). New York, NY: North-Holland Pub. Co. doi: 10.1016/s0169-7161(80)01011-5

Mason, R. L., Chou, Y.-M., & Young, J. C. (2001). Applying Hotelling's T^2 statistic to batch processes. *Journal of Quality Technology, 33*(4), 466-479. doi: 10.1080/00224065.2001.11980105

Mostajeran, A., Iranpanah, N., & Noorossana, R. (2016). A new bootstrap based algorithm for Hotelling’s T2 multivariate control chart. *Journal of Sciences, Islamic Republic of Iran, 27*(3), 269-278. Retrieved from https://jsciences.ut.ac.ir/article_57658.html

Noorossana, R., Fathizadan, S., & Nayebpour, M. (2015). EWMA control chart performance with estimated parameters under non-normality. *Quality and Reliability Engineering International, 32*(5), 1637-1654. doi: 10.1002/qre.1896

Park, H.-I. (2009). Median control charts based on bootstrap method. *Communications in Statistics – Simulation and Computation, 38*(3), 558-570. doi: 10.1080/03610910802585824

Phaladiganon, P., Kim, S. B., Chen, V. C., Baek, J.-G., & Park, S.-K. (2011). Bootstrap-based T^2 multivariate control charts. *Communications in Statistics – Simulation and Computation, 40*(5), 645-662. doi: 10.1080/03610918.2010.549989

Phaladiganon, P., Kim, S. B., Chen, V. C., & Jiang, W. (2013). Principal component analysis-based control charts for multivariate nonnormal distributions.

Expert Systems with Applications, *40*(8), 3044-3054. doi: 10.1016/j.eswa.2012.12.020

Polansky, A. M. (2005). A general framework for constructing control charts. *Quality and Reliability Engineering International*, *21*(6), 633-653. doi: 10.1002/qre.680

Psarakis, S., Vyniou, A. K., & Castagliola, P. (2014). Some recent developments on the effects of parameter estimation on control charts. *Quality and Reliability Engineering International*, *30*(8), 1113-1129. doi: 10.1002/qre.1556

Saleh, N. A., Mahmoud, M. A., & Abdel-Salam, A.-S. G. (2013). The performance of the adaptive exponentially weighted moving average control chart with estimated parameters. *Quality and Reliability Engineering International*, *29*(4), 595-606. doi: 10.1002/qre.1408

Saleh, N. A., Zwetsloot, I. M., Mahmoud, M. A., & Woodall, W. H. (2016). CUSUM charts with controlled conditional performance under estimated parameters. *Quality Engineering*, *28*(4), 402-415. doi: 10.1080/08982112.2016.1144072

Seppala, T., Moskowitz, H., Plante, R., & Tang, J. (1995). Statistical process control via the subgroup bootstrap. *Journal of Quality Technology*, *27*(2), 139-153. doi: 10.1080/00224065.1995.11979577